

Ji H. Hwang · Young T. Oh · Won T. Kwon  
Chong N. Chu

## In-process estimation of radial immersion ratio in face milling using cutting force

Received: 19 March 2002 / Accepted: 24 July 2003 / Published online: 10 July 2003  
© Springer-Verlag London Limited 2003

**Abstract** In order to prevent tool breakage in milling, maximum total cutting force is regulated at a specific constant level, or threshold, through feed rate control. Since the threshold is a function of the immersion ratio, an estimation of the immersion ratio is necessary to flexibly determine the threshold. In this paper, a method of in-process estimation of the radial immersion ratio in face milling is presented. When an insert finishes sweeping, a sudden drop in cutting forces occurs. These force drops are equal to the cutting forces that act upon a single insert at the swept cutting angle and they can be acquired from cutting force signals in the feed and cross-feed directions. Average cutting forces per tooth period can also be calculated from the cutting force signals in two directions. The ratio of cutting forces acting upon a single insert at the swept angle of cut and the ratio of average cutting forces per tooth period are functions of the swept angle of cut and the ratio of radial to tangential cutting force. Using these parameters, the radial immersion ratio is estimated. Various experiments are performed to verify the proposed method. The results show that the radial immersion ratio can be estimated by this method regardless of other cutting conditions.

**Keywords** Cutting force · In-process estimation · Radial immersion ratio

### Nomenclature

$F_T, F_R$  tangential and radial forces  
 $F_X, F_Y$  cutting forces in feed direction and cross feed direction

$dF_X, dF_Y$  cutting force differences before and after the immersion angle in X and Y direction  
 $K_s$  specific cutting pressure  
 $a$  depth of cut  
 $r$  ratio between tangential force and radial force  
 $s_t$  feed per tooth  
 $\phi$  instantaneous angle of cut  
 $\phi_s$  swept angle of cut  
 $\phi_T$  tooth spacing angle  
 $w$  radial width of cut  
 $R$  cutter radius  
 $z$  number of inserts

### 1 Introduction

The need for monitoring the cutting process is a well-known user requirement for intelligent manufacturing systems. Among the parameters for monitoring the cutting process, cutting force signal is known to be the most accurate. When monitoring the cutting process via the cutting force, a cutting force limit value is required to distinguish an abnormal state, such as tool breakage or overload, from a normal state. This predetermined value is called the threshold value. Since the threshold is a function of cutting parameters, identification of cutting parameters is necessary to accurately set the threshold. In the face milling process, the radial depth of cut or radial immersion ratio is the parameter that most affects the determination of the threshold. Tool breakage occurs when the tension on a tooth exceeds the maximum tensile stress of the tooth. To prevent tool breakage, the maximum stress on a tooth must be kept below a certain value. The threshold is the sum of maximum allowable forces on each tooth. As the immersion ratio changes, the number of teeth involved in cutting and the sum of the maximum allowable forces (the threshold) also change. If the number of teeth participating in cutting increases, the cutting force acting on a tooth decreases. Therefore, constraining the maximum total cutting

J. H. Hwang · C. N. Chu (✉)  
School of Mechanical and Aerospace Engineering,  
Seoul National University, 151-742 Seoul, Korea  
E-mail: cnchu@snu.ac.kr

Y. T. Oh  
Department of Mechanical Engineering,  
Ansan College of Technology, 425-792 Kyungki, Korea

W. T. Kwon  
Department of Mechanical and Information Engineering,  
University of Seoul, 130-743 Seoul, Korea

force, regardless of the number of teeth, results in a decrease of productivity. To determine the threshold according to the number of teeth involved in cutting, the radial immersion ratio must also be known.

Estimation of cutting conditions during machining has been made in the past. Altintas and Yellowley [1] developed an algorithm to identify both the axial depth and radial width of cut based on two orthogonal force measurements. A cubic polynomial was used to establish the immersion ratio prediction model. Altintas and Yellowley [2,6] also developed another algorithm based on the mean and time varying components of the measured force. They showed that the immersion ratio can be represented by the ratio of the mean squared value of the instantaneous cutting force to the square of the quasi-mean resultant force. Tarn and Tomizuka [3] measured the time during which a tool is engaged in a work piece to estimate the immersion ratio using the cutting force. Choi and Yang [4] used the trend of cutting force variation to estimate the radial and axial immersion ratios. Lee [5] used both cutting force and tool engagement time in the work piece to identify the immersion ratio even when more than two inserts were involved in cutting.

This paper presents an on-line estimation of the radial immersion ratio in face milling. When an insert finishes sweeping, a sudden drop of force occurs. The force drop is equal to the cutting force that acts upon an insert at the swept angle of cut and can be acquired from the cutting force signals in the feed and cross-feed directions. The ratio of cutting forces acting on an insert at the swept angle of cut and the ratio of average cutting forces per tooth period are functions of the swept angle of cut and the ratio of radial to tangential cutting forces. Using these parameters, the radial immersion ratio is estimated. Experiments are performed for axial depths of cut, cutter diameters, spindle speeds and number of inserts.

## 2 Algorithm for estimation of radial immersion ratio

### 2.1 Equation for estimation of radial immersion ratio

The tangential force,  $F_T$ , and the radial force,  $F_R$ , can be represented by feed per tooth,  $s_t$ , depth of cut,  $a$ , specific cutting pressure,  $K_s$ , the ratio between  $F_T$  and  $F_R$ ,  $r$ , and the instantaneous angle of cut,  $\phi$ .

$$F_T(\phi) = K_s a s_t \sin(\phi) \quad (1)$$

$$\begin{aligned} F_R(\phi) &= r F_T \\ &= r K_s a s_t \sin(\phi) \end{aligned} \quad (2)$$

The cutting forces in the feed direction,  $F_X(\phi_s)$ , and cross-feed direction,  $F_Y(\phi_s)$ , on an insert at the swept angle of cut,  $\phi_s$ , can be expressed as,

$$\begin{aligned} F_X(\phi_s) &= F_T \cos(\phi_s) + F_R \sin(\phi_s) \\ &= K_s a s_t \sin(\phi_s) \cos(\phi_s) + r K_s a s_t \sin(\phi_s) \sin(\phi_s) \end{aligned} \quad (3)$$

$$\begin{aligned} F_Y(\phi_s) &= F_R \cos(\phi_s) - F_T \sin(\phi_s) \\ &= r K_s a s_t \sin(\phi_s) \cos(\phi_s) - K_s a s_t \sin(\phi_s) \sin(\phi_s) \end{aligned} \quad (4)$$

Cutting forces,  $F_X(\phi_s)$  and  $F_Y(\phi_s)$ , are functions of the cutting condition, such as depth of cut, feed per tooth and radial immersion angle. The ratio of  $F_Y(\phi_s)$  to  $F_X(\phi_s)$  is a function of the swept angle of cut (or the immersion angle),  $\phi_s$ , and the ratio of the tangential force to radial force,  $r$ .

$$\frac{F_Y(\phi_s)}{F_X(\phi_s)} = \frac{r - \tan(\phi_s)}{1 + r \tan(\phi_s)} \quad (5)$$

Equation 5 can be rewritten as,

$$\phi_s = \tan^{-1} \frac{r - \frac{F_Y(\phi_s)}{F_X(\phi_s)}}{1 + r \frac{F_Y(\phi_s)}{F_X(\phi_s)}} \quad (6)$$

and the relation between immersion ratio and immersion angle is [1],

$$\begin{aligned} \text{immersion ratio} &= \frac{w}{R} \\ &= 1 - \cos(\phi_s) \end{aligned} \quad (7)$$

where  $w$  is the radial width of cut and  $R$  is the cutter radius.

The relation between the immersion angle and the ratio of  $F_Y(\phi_s)$  to  $F_X(\phi_s)$  is plotted in Fig. 1. As can be seen in the figure, when the ratio of  $F_Y(\phi_s)$  to  $F_X(\phi_s)$  is constant, the immersion angle (or the swept angle of cut) increases as the ratio  $r$  increases. Therefore, even when the measured forces,  $F_Y(\phi_s)$  and  $F_X(\phi_s)$ , are the same, the immersion angle can be estimated differently if the magnitude of  $r$  is different. When the magnitude of  $r$  is constant, the estimated immersion angle becomes larger as the ratio of measured cutting forces increases. As a result, the immersion angle and the ratio between cutting

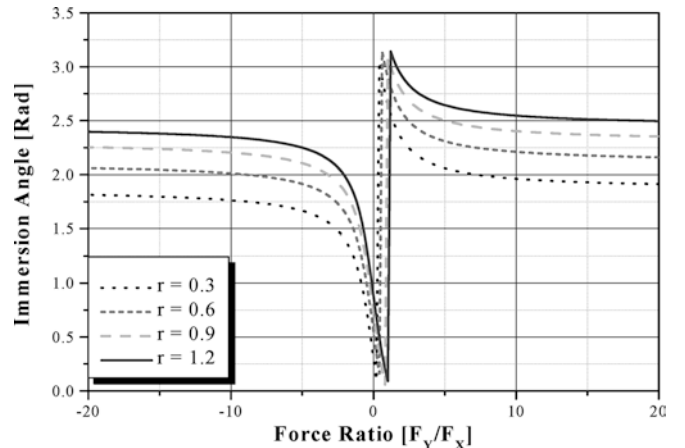


Fig. 1 Relationship between the immersion angle ( $\phi_s$ ) and the ratio of the cutting forces ( $F_Y/F_X$ ) on an insert

forces,  $F_Y(\phi_s)$  and  $F_X(\phi_s)$ , should be estimated simultaneously to identify both parameters accurately.

Another equation that can be used for the estimation of the immersion angle is the average cutting force per tooth,

$$F_{aX}(\phi_s) = \frac{1}{\phi_T} \int_0^{\phi_s} F_X(\phi) d\phi$$

$$= \frac{K_s a s_T z}{8\pi} [(1 - \cos(2\phi_s)) + r_{av}(2\phi_s - \sin(2\phi_s))] \quad (8)$$

$$F_{aY}(\phi_s) = \frac{1}{\phi_T} \int_0^{\phi_s} F_Y(\phi) d\phi$$

$$= \frac{K_s a s_T z}{8\pi} [r_{av}(1 - \cos(2\phi_s)) - (2\phi_s - \sin(2\phi_s))] \quad (9)$$

where  $\phi_T = \frac{2\pi}{z}$ ,  $z$  is the number of inserts and  $r_{av}$  is the average value of  $r$  between 0 and  $\phi_s$ .

The ratio of  $F_{aY}$  to  $F_{aX}$  is also a function of  $\phi_s$  and  $r$ . Dividing  $F_{aY}(\phi_s)$  by  $F_{aX}(\phi_s)$  and rearranging the equation for  $r_{av}$  yields,

$$\frac{F_{aY}(\phi_s)}{F_{aX}(\phi_s)} = \frac{r_{av}(1 - \cos(2\phi_s)) - (2\phi_s - \sin(2\phi_s))}{(1 - \cos(2\phi_s)) + r_{av}(2\phi_s - \sin(2\phi_s))} \quad (10)$$

$$r_{av} = \frac{(2\phi_s - \sin(2\phi_s)) + \frac{F_{aY}(\phi_s)}{F_{aX}(\phi_s)}(1 - \cos(2\phi_s))}{(1 - \cos(2\phi_s)) - \frac{F_{aY}(\phi_s)}{F_{aX}(\phi_s)}(2\phi_s - \sin(2\phi_s))} \quad (11)$$

$$r = ar_{av} + b \quad (12)$$

where  $a$  and  $b$  are constants.

Equation 11 expresses the relation between  $r_{av}$ ,  $\phi_s$  and the ratio of  $F_{aY}$  to  $F_{aX}$  and is plotted in Fig. 2. If the ratio of  $F_{aY}$  to  $F_{aX}$  is constant, the immersion angle  $\phi_s$  is estimated to be larger when the magnitude of  $r_{av}$  is larger as shown in Fig. 2. If  $r_{av}$  is constant, the immersion ratio

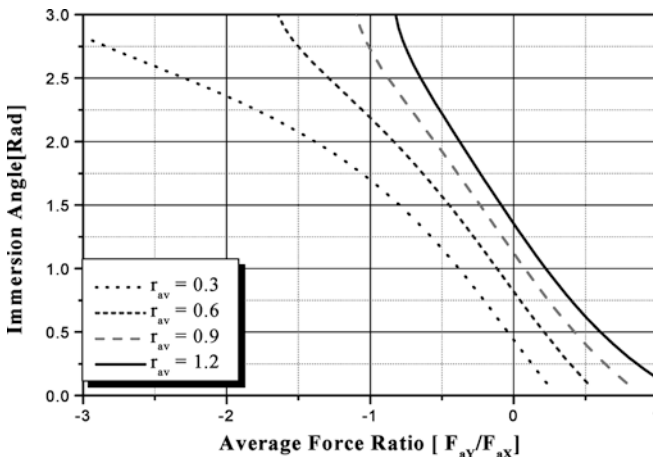


Fig. 2 Relationship between the immersion angle ( $\phi_s$ ) and the ratio of the average forces ( $F_{aY}/F_{aX}$ ) on an insert

is estimated to be smaller when the ratio of  $F_{aY}$  to  $F_{aX}$  is larger. The relation between  $r$  and  $r_{av}$  is assumed to be linear in Eq. 12 and will be proved experimentally later.

Even though we have three equations for three variables in Eqs. 6, 11 and 12 the problem cannot be solved analytically. A numerical method is used to obtain solutions for  $r$ ,  $r_{av}$  and the immersion angle  $\phi_s$ . The procedure to solve the problem is as follows: First, an initial value of  $r$  between 0 and 1 is arbitrarily determined. Then the immersion angle  $\phi_s$  can be calculated from Eq. 6. If the magnitude of the initial  $r$  is smaller than the magnitude of the real  $r$ , the estimated  $\phi_s$  is smaller than the real  $\phi_s$  as shown in Fig. 1. In the same manner, if the initial  $r$  is larger than the real  $r$ , then the estimated  $\phi_s$  is larger than the real  $\phi_s$ . Next, the estimated  $\phi_s$  is substituted into Eq. 11 to find  $r_{av}$ , which is in turn substituted in Eq. 12 to find  $r$ . The magnitude of  $r$  obtained from Eq. 12 is between the real  $r$  and initial  $r$ . The newly obtained  $r$  is substituted again into Eq. 6 to calculate  $\phi_s$ . This iterative calculation is repeated until  $r$  converges to a certain value. As a result, the real  $\phi_s$  and  $r$  can be estimated from the measured forces in the feed and cross-feed directions by iterative calculation.

## 2.2 Convergence of $r$ by iterative calculation

In the previous section, it was assumed that the magnitude of the newly calculated  $r$  was between the initial  $r$  and the real  $r$ . If  $r$  is not between the initial  $r$  and real  $r$ , it will not converge by iterative calculation. Hence, the convergence of  $r$  has to be proven for the existence of a solution. The existence of a solution can be proved by comparing the derivatives of Eqs. 6 and 11. The derivative of  $\phi_s$  by  $r$  is calculated from Eqs. 6, 11 and 12 and is shown in Eqs. 13 and 14.

$$\frac{d\phi_s}{dr} = \frac{1}{1+r^2} \quad (13)$$

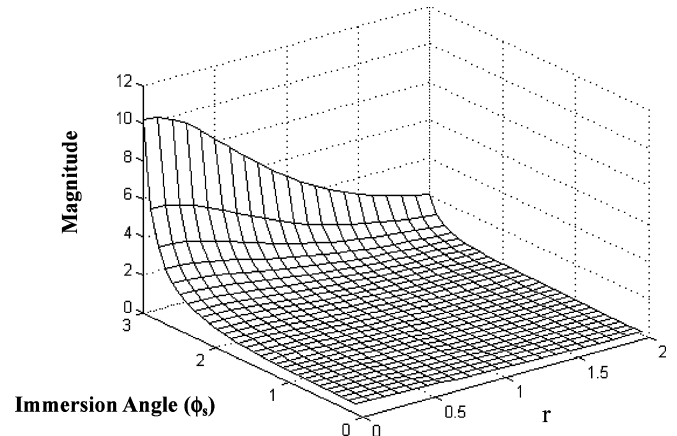


Fig. 3 Difference between the derivatives of immersion angle by  $r$  calculated from instant cutting forces at the swept angle of cut and from average cutting forces

$$\begin{aligned} \frac{d\phi_s}{dr} &= \frac{d\phi_s}{dr_{av}} \frac{dr_{av}}{dr} \\ &= \frac{1 \csc(\phi_s) \{-1 - 2\phi_s^2 + \cos(2\phi_s) + 2\phi_s \sin(2\phi_s)\}}{a 4(1+r^2)(\phi_s \cos(\phi_s) - \sin(\phi_s))} \end{aligned} \quad (14)$$

The difference between Eqs. 13 and 14 is shown in Fig. 3 as a function of immersion angle and  $r$  when  $a=1$ . As can be seen in Fig. 3, the difference is always positive, which means that the variance of  $\phi_s$  according to  $r$  in Eq. 14 is always larger than the variance of  $\phi_s$  according to  $r$  in Eq. 13 if  $a$  is equal or smaller than 1. Therefore the new ratio  $r$ , calculated by substituting the immersion angle in Eq. 12, is between the real  $r$  and the initial  $r$ . As the iterative calculation proceeds, the new  $r$  is always located between the previous  $r$  and the real  $r$ . In this manner, the estimated  $r$  converges. It will be proven experimentally that the magnitude of  $a$  is smaller than unity.

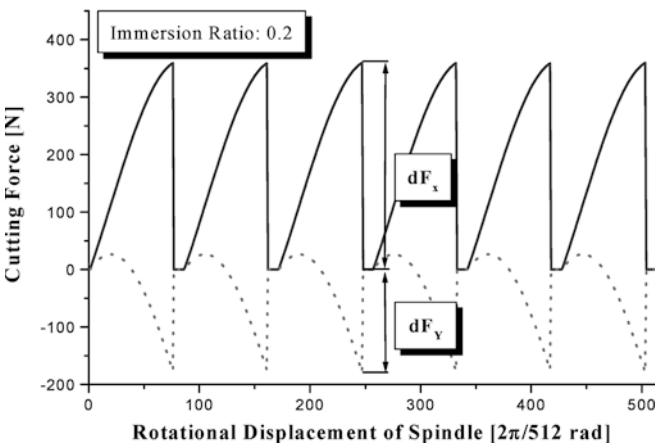


Fig. 4 Pattern of simulated cutting forces when one insert participates in cutting

### 2.3 Cutting force on an insert

The cutting force on an insert at the immersion angle has to be measured to estimate immersion angle using Eqs. 6 and 11. A method for separating those forces from the measured cutting forces is given in the following section.

#### 2.3.1 Separation of cutting force on an insert when only one insert participates in machining

When a cutter with several inserts cuts, it may be that only one insert is involved in cutting. Figure 4 shows the simulated cutting force when only one insert at a time is cutting during face milling. The cutting force increases from 0 N to its maximum value, after which it drops to 0 N again. The discontinuity of the cutting force occurs at the immersion angle. In this case the magnitude of the force drop represents the cutting force on an insert at the swept angle of cut.

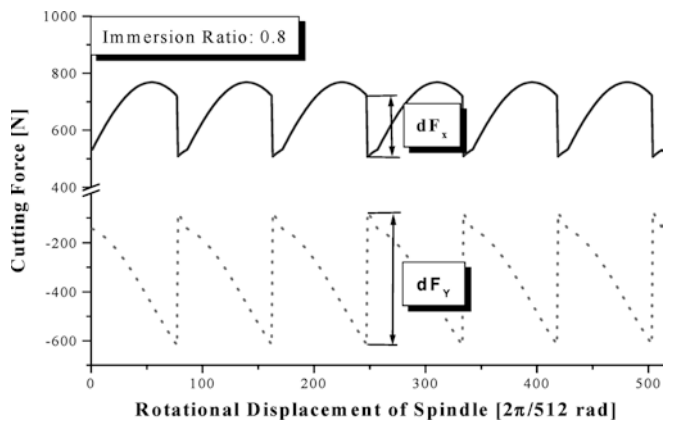
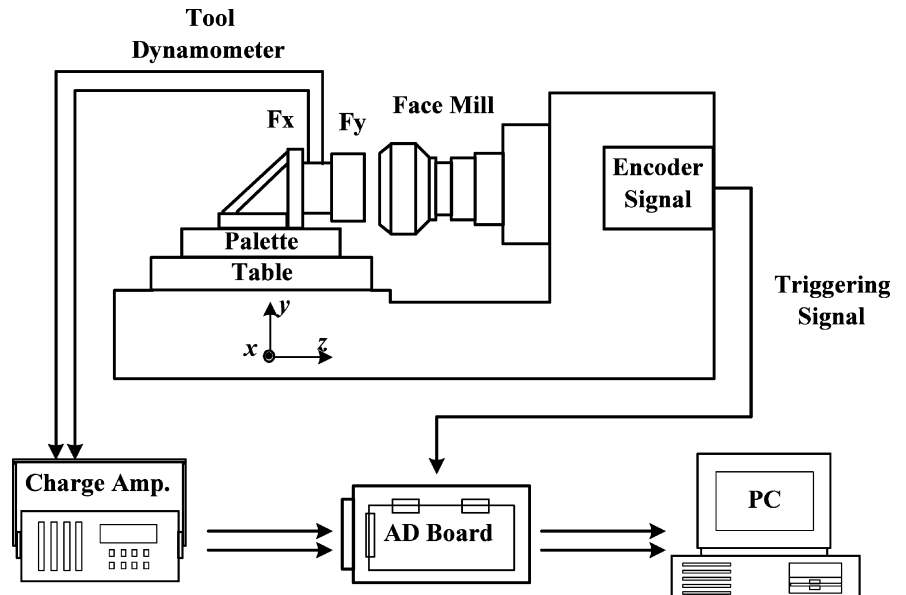


Fig. 5 Pattern of simulated cutting forces when two inserts participate in cutting

Fig. 6 Schematics of experimental setup



$$dF_X = F_X(\phi_s) \quad (15)$$

$$dF_Y = F_Y(\phi_s) \quad (16)$$

where  $dF_X$  and  $dF_Y$  are cutting force differences before and after the immersion angle in  $X$  and  $Y$  direction, respectively.

### 2.3.2 Separation of cutting force on a single insert when more than two inserts participate in Cutting

Figure 5 shows the simulated cutting force when more than two inserts participate in cutting at the same time. In this case, the cutting force on each insert is summed to represent the total cutting force. When one insert stops cutting at the immersion angle, a force drop occurs. The magnitude of the force drop is equal to the cutting force on an insert just before it exits the work piece. Since the other inserts are cutting when one insert exits, total cutting force is not 0.

$$\begin{aligned} dF_X &= \sum_{k=1}^N F_X[\phi_s - (k-1)\phi_T] - \sum_{k=2}^N F_X[\phi_s - (k-1)\phi_T] \\ &= F_X(\phi_s) \end{aligned} \quad (17)$$

$$\begin{aligned} dF_Y &= \sum_{k=1}^N F_Y[\phi_s - (k-1)\phi_T] - \sum_{k=2}^N F_Y[\phi_s - (k-1)\phi_T] \\ &= F_Y(\phi_s) \end{aligned} \quad (18)$$

## 3 Experiments and results

### 3.1 Experimental setup

A schematic representation of the experimental setup is shown in Fig. 6. Experiments were carried out on a

horizontal machining center (Daewoo ACE-H40). The cutting force was measured by a piezo-type tool dynamometer (Kistler 9257B) and the measured force was amplified using a charge amplifier (Kistler 5011). A low-pass filter in the charge amplifier with 300 Hz cut off frequency was used to filter out the high frequency noise. An A/D converter (Real Time Device A/D 2210) and a PC were used for data processing. Sampling of the force components was controlled by the signal from the encoder attached to the end of the spindle. In these experiments, 512 pulses per revolution were produced by the encoder. A face milling cutter with a 100 mm diameter was used to cut carbon steel SM45C (AISI 1045) and aluminium alloy 6061 and the inserts were TiCN coated carbide grade (TaeguTec SPKN1203EDR KT700). The cutting conditions are given in Table 1.

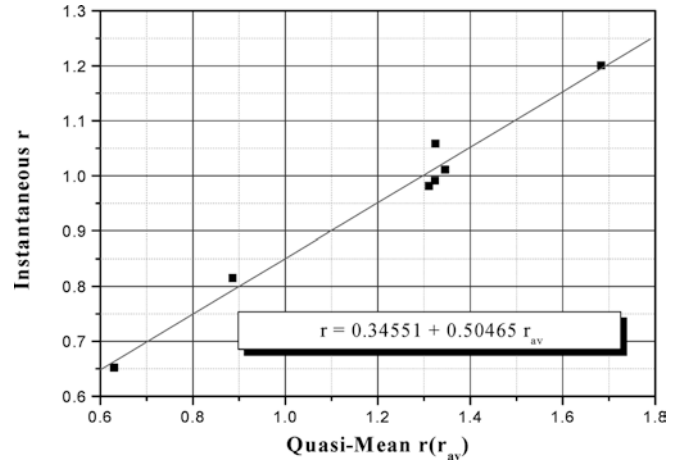


Fig. 7 Relationship between quasi-mean and instantaneous  $r$  at the immersion angle

Table 1 Cutting conditions for the experiments

	Spindle speed (RPM)	Cutter diameter (mm)	Feed per tooth (mm/min)	Immersion ratio (%)	No. of inserts	Axial depth of cut (mm)	Material
Cutting force variation	200	100	0.15	20–80	3	1.5	SM45C
	300	100	0.15	20–80	3	1.5	SM45C
	400	100	0.15	20–80	3	1.5	SM45C
Depth of cut variation	300	100	0.15	20–80	3	1	SM45C
	300	100	0.15	20–80	3	1.5	SM45C
	300	100	0.15	20–80	3	2	SM45C
Cutter diameter variation	300	50	0.15	20–80	3	1.5	SM45C
	300	100	0.15	20–80	3	1.5	SM45C
	300	100	0.15	20–80	3	1.5	SM45C
No. of inserts variation	200	100	0.15	20–80	2	1	SM45C
	200	100	0.15	20–80	3	1	SM45C
	200	100	0.15	20–80	6	1	SM45C
Feed-rate variation	300	100	0.1	20–80	3	1.5	SM45C
	300	100	0.15	20–80	3	1.5	SM45C
	300	100	0.2	20–80	3	1.5	SM45C
Material	300	100	0.15	20–80	3	1.5	SM45C
	300	100	0.15	20–80	3	1.5	Al
Material with continuously varying immersion ratio	200	100	0.15	20–80	6	1	SM45C

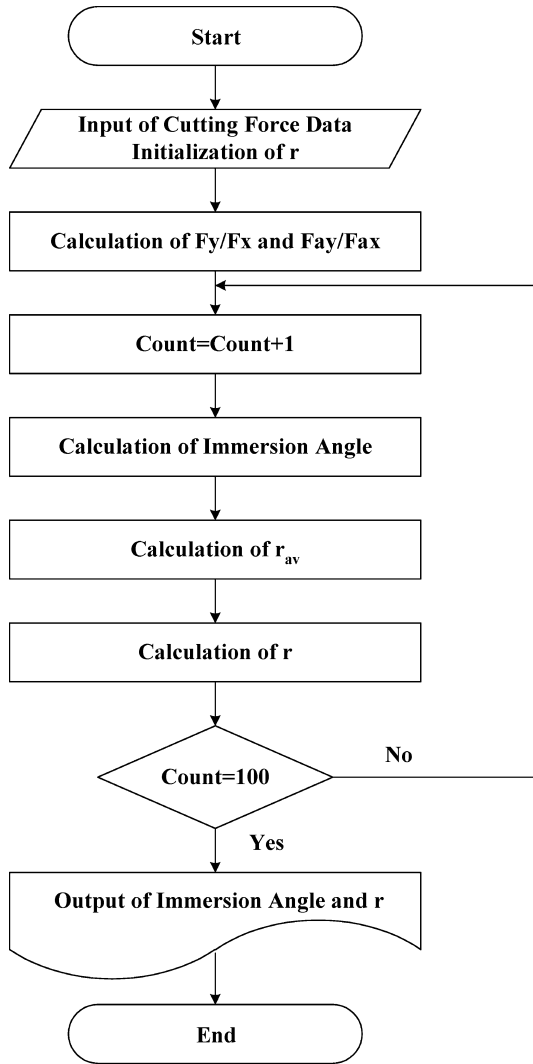


Fig. 8 Flowchart of the algorithm for estimation of radial immersion ratio

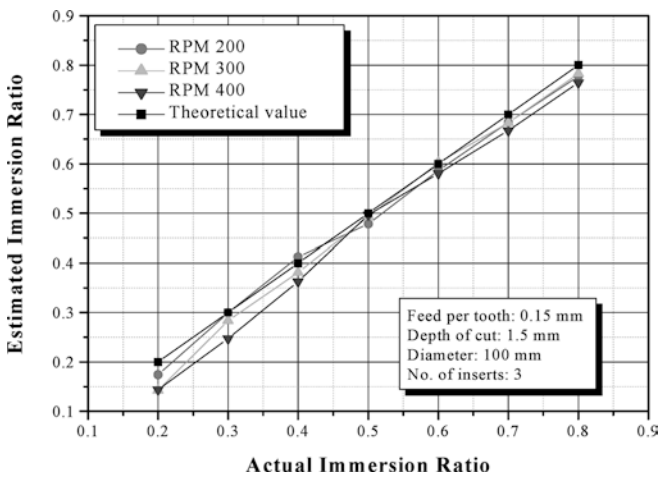


Fig. 9 Estimation of immersion ratio according to spindle speed

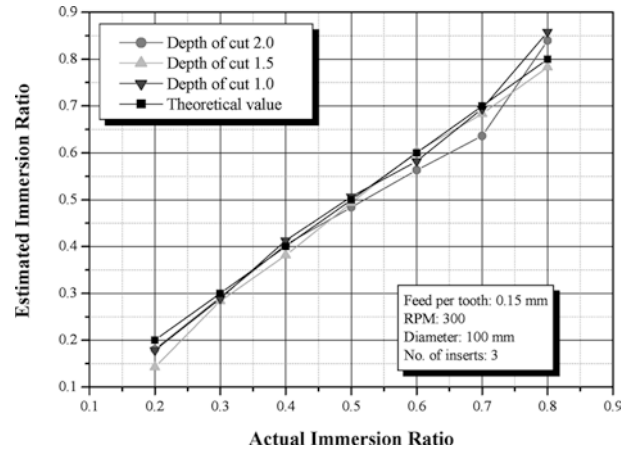


Fig. 10 Estimation of immersion ratio according to axial depth of cut

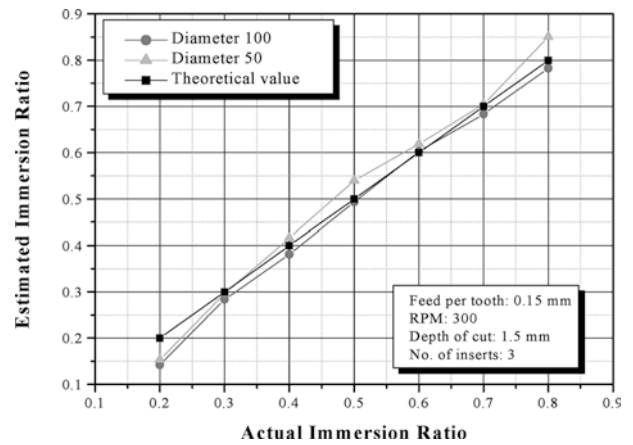


Fig. 11 Estimation of immersion ratio according to cutter diameter

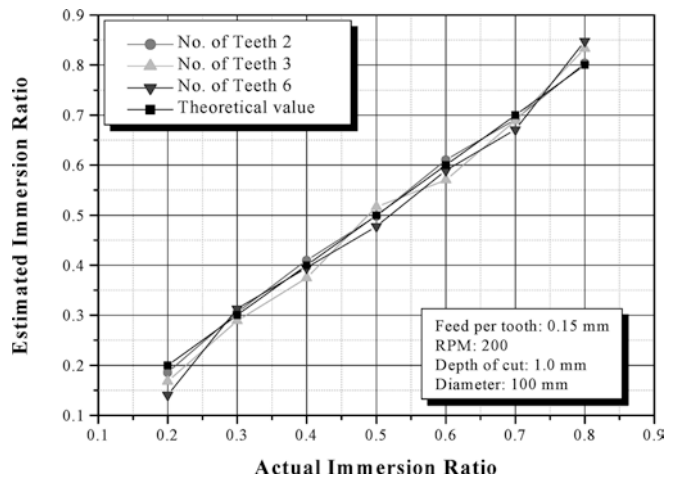


Fig. 12 Estimation of immersion ratio according to number of inserts

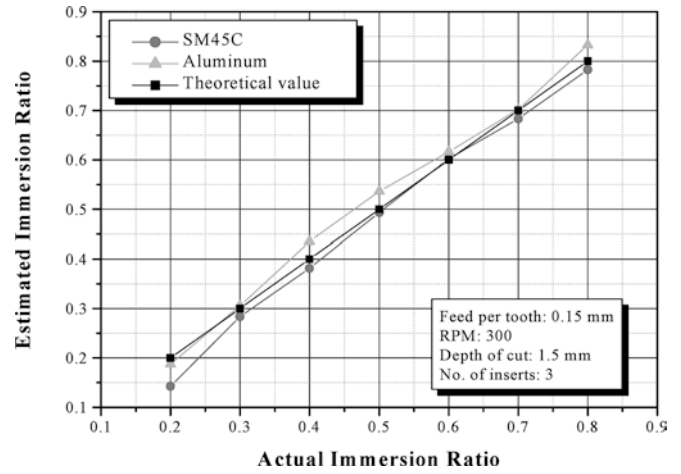
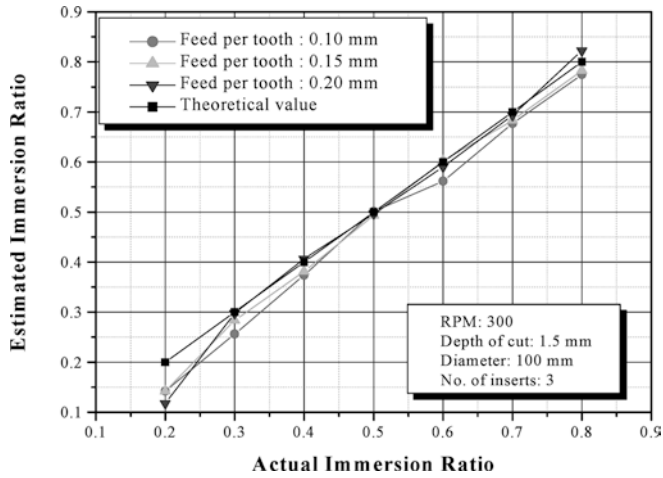
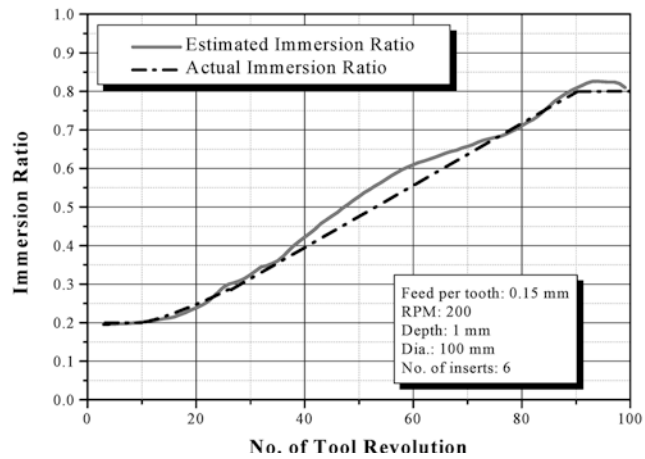
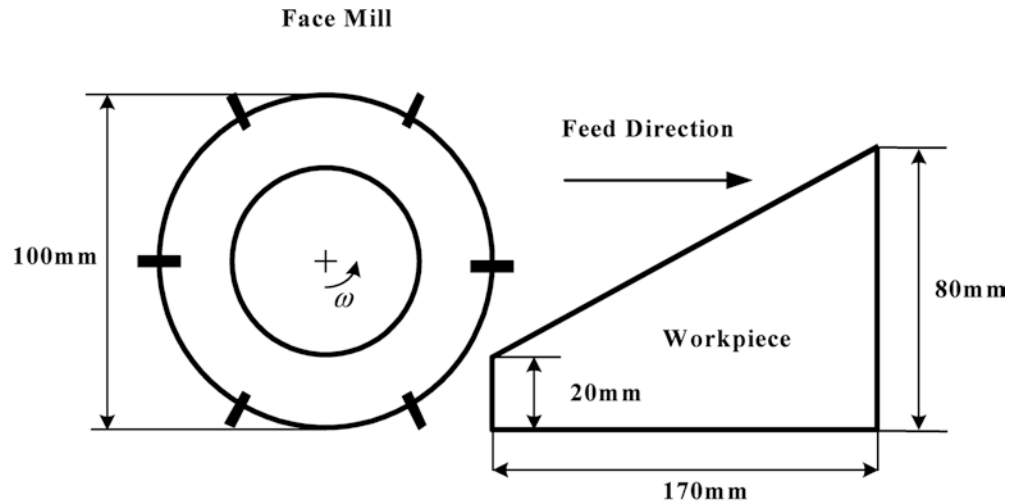


Fig. 13 Estimation of immersion ratio according to feed per tooth

Fig. 14 Estimation of immersion ratio according to material

Fig. 15 a Geometry of work piece b estimation of continuously varying immersion ratio



## 3.2 Experimental results

### 3.2.1 Relation between average cutting force and cutting force at immersion angle

It was proved that  $r$  converges by iterative calculation if the magnitude of  $a$  in Eq. 12 was equal to or smaller than 1. We will prove that the relation between  $r$  and  $r_{av}$  can be fitted to a linear function and the constant  $a$  is smaller than unity. The relation is experimentally obtained and given in Fig. 7. As shown in the figure, it can be fitted to a linear function and the magnitude of  $a$  is 0.50465. Since  $r$  is smaller than 1, the convergence of  $r$  by iterative calculation is guaranteed (see flowchart in 8).

### 3.2.2 Estimation of immersion ratio

Experiments were carried out under various cutting conditions: various spindle speeds, depth of cuts, cutter diameters, number of inserts, feeds per tooth and with different work piece materials. These cutting conditions are given in Table 1. The results are shown in Figs. 9, 10, 11, 12, 13 and 14. The estimated immersion ratio is within a 10% error range regardless of the cutting conditions. Compared with other immersion ratios, the error is relatively large when  $r$  is 0.2. This is attributed to the edge effect or parasitic force [2]. The authors measured the edge radius of the new insert and the radius was 70–80  $\mu\text{m}$ . The cutting force is assumed to be linear to the feed per tooth in Eqs. 1 and 2. Because of the worn part at the end of the insert, the cutting force is not proportional to the feed per tooth when the feed per tooth is small, which causes the discrepancy between the calculated and measured cutting force. The discrepancy becomes larger as the feed per tooth becomes smaller. As a result, the error of the estimated immersion ratio based on the linear cutting force becomes larger as the feed per tooth becomes smaller, which explains the relatively large error when  $r$  is 0.2. The experiments were also executed on a work piece with a continuously varying immersion ratio. The results in Fig. 15 show that proposed algorithm works well.

## 4 Conclusions

The force drop at the end of the immersion angle is used to determine the force applied on an insert in the feed and cross-feed direction. The ratio between the feed direction and the cross-feed direction forces is also expressed as a function of immersion angle and the ratio between the tangential and radial direction force. The average forces in the feed and cross feed direction are calculated from the measured cutting forces and are expressed as a function of immersion ratio and the ratio between the tangential and radial forces. The immersion ratio and the ratio between the tangential and radial direction force is obtained from the measured cutting force using the relation between cutting forces, immersion angle and the ratio between feed and cross-feed direction forces. An iterative calculation method is used to solve this problem, which is unsolvable by analytical methods. The proposed algorithm works well within 10% error range regardless of cutting conditions: cutting speed, depth of cut, feed per tooth, cutter diameter, number of inserts and work piece materials. The relatively large estimation error when the immersion ratio is small is attributed to the edge effect or parasitic force at the end of the insert. It is also proved that the algorithm is reliable during machining the work piece with a continuously varying immersion ratio.

## References

1. Altintas Y, Yellowley I (1987) The identification of radial width and axial depth of cut in peripheral milling. *Int J Mach* 27(3):367–381
2. Altintas Y, Yellowley I (1989) In-process detection of tool failure in milling using cutting force models. *Transactions ASME, J Eng Ind* 111(2):149–157
3. Tarn JH, Tomizuka M (1989) On-line monitoring of tool and cutting conditions in milling. *Transactions ASME, J Eng Ind* 111(3):206–212
4. Choi JG, Yang MY (1999) In-process prediction of cutting depth in end milling. *Int J Mach* 39(5):705–721
5. Lee SI (1998) Prediction of radial immersion ratio in face milling. M. S. Thesis, Seoul National University
6. Altintas Y, Yellowley I, Tlustý J (1988) The detection of tool breakage in milling operation. *Transactions ASME, J Eng Ind* 110(3):271–277